



Marine Phytoplankton Stoichiometry Mediates Nonlinear Interactions Between Nutrient Supply, Temperature, and Atmospheric CO₂

Allison R. Moreno¹, George I. Hagstrom², Francois W. Primeau³, Simon A. Levin², Adam C.
Martiny^{1,3*}

Affiliations:

1. Department of Ecology and Evolutionary Biology, University of California, Irvine, California 92697, USA.
2. Department of Ecology and Evolutionary Biology, Princeton University, Princeton, New Jersey 08544, USA.
3. Department of Earth System Science, University of California, Irvine, California 92697, USA.

*Corresponding Author
amartiny@uci.edu

Keywords: Redfield Ratio, Traits, Carbon Cycling,

Working title: Feedbacks Between Marine Stoichiometry, Environment, and Atmospheric CO₂



Abstract

Marine phytoplankton stoichiometry links nutrient supply to marine carbon export. Deviations of phytoplankton stoichiometry from Redfield proportions (106C:1P) could therefore have a significant impact on carbon cycling, and understanding which environmental factors drive these deviations may reveal new mechanisms that regulate the carbon cycle. To explore the links between environmental conditions, stoichiometry, and carbon cycling, we compared four different models for variations in phytoplankton C:P: a fixed Redfield model, a model with C:P given as a function of surface phosphorus concentration ([P]), a model with C:P given as a function of temperature, and a new multi-environmental model that predicts C:P as a function of light, temperature, and [P]. These stoichiometric models were embedded into a box model of the ocean circulation, which resolves the three major ocean biomes (high-latitude, subtropical gyres, and iron-limited tropical upwelling regions). Contrary to the expectation of a monotonic relationship between surface nutrient drawdown and carbon export, we found that lateral nutrient transport from lower C:P tropical waters to high C:P subtropical waters could cause carbon-export to decrease with increased tropical nutrient utilization. Temperature is thought to be one of the primary drivers of changes in atmospheric $p\text{CO}_2$ ($p\text{CO}_{2,\text{atm}}$) across glacial/interglacial periods, and it has been hypothesized that a positive feedback between temperature and $p\text{CO}_{2,\text{atm}}$ will play an important role in anthropogenic climate change, with changes in the biological pump playing at most a secondary role. Here we show that environmentally driven shifts in stoichiometry make the biological pump more influential, and may reverse the expected negative relationship between temperature and $p\text{CO}_{2,\text{atm}}$. In the temperature-only model changes in tropical temperature have more impact on the $\Delta p\text{CO}_{2,\text{atm}}$ (~41 ppm) compared to subtropical temperature (~4.5 ppm). Our multi-environmental model produced a decline in $p\text{CO}_{2,\text{atm}}$ of ~46 when temperature spanned a change of 10°C. Thus, we find that variation in marine phytoplankton stoichiometry and its environmental controlling factor can lead to counterintuitive controls on $p\text{CO}_{2,\text{atm}}$, suggesting the need for further studies of ocean C:P and the impact on ocean carbon cycling.



1 Introduction

The discovery of large-scale deviations of phytoplankton stoichiometry from the Redfield ratio in the past decade (Martiny et al., 2013a, 2013b; Weber and Deutsch, 2010) has significant consequences for our understanding of the biological carbon pump and global carbon cycling (Galbraith and Martiny, 2015). Traditionally, the biological pump is thought to be controlled by a combination of the vertical nutrient flux and nutrient utilization efficiency (Sarmiento and Toggweiler, 1984). However, variable elemental stoichiometry of exported organic material ($C:P_{export}$) adds a new biological dimension to this problem and may lead to higher than currently expected carbon export in subtropical regions (Emerson, 2014; Teng et al., 2014). Global carbon export has been estimated to range between 5 and 12 Pg C/year (Boyd and Trull, 2007; Henson et al., 2011), but these projections have yet to incorporate the controls on $C:P_{export}$. Variation in $C:P_{export}$ from Redfield proportions can be linked to environmental conditions. There are two leading environmental parameters thought to control $C:P_{export}$; nutrients, predominantly phosphate concentrations, and temperature. Galbraith and Martiny (2015) used a simple three-box model to show that variable stoichiometry driven by phosphate availability could enhance the efficiency of the biological pump in the low-latitude ocean (Galbraith and Martiny, 2015). In contrast, Yvon-Durocher (2015) used a meta-analysis of global temperature and stoichiometric ratios to propose that C:P increased 2.6-fold from 0° C to 30° C. Thus, it is currently unclear if differences in nutrient supply, temperature, or some combination of them, control the global variation in C:P of plankton and exported material,

There are two important ingredients missing from published studies that could alter the interactions among phytoplankton stoichiometry, carbon export, and atmospheric pCO_2 ($pCO_{2,atm}$). The first is the presence of two unique low-latitude biomes, namely the iron-stressed equatorial upwelling regions and the macronutrient-depleted subtropical gyres. Iron deposition in the tropical upwelling zones strongly controls nutrient drawdown and the degree of macronutrient limitation. In direct observations and inverse model analyses, these two biome types appear to have unique elemental compositions, which leads to relatively increased rates of export from oligotrophic gyres in comparison to equatorial upwelling regions (DeVries and Deutsch, 2014; Martiny et al., 2013a; Teng et al., 2014). Thus, in order to properly represent global variations in surface plankton C:P and carbon export, it is essential to separately model both macronutrient limited subtropical gyres and iron-limited equatorial upwelling zones.

The second missing ingredient is that environmental factors beyond nutrient availability may impact the elemental composition of surface plankton and $C:P_{export}$. Temperature, irradiance, and nutrient concentrations are important environmental factors, which influence the physiology and stoichiometry of phytoplankton. However, surveys of phytoplankton C:P are insufficient to distinguish between the separate effects of each factor on C:P due to strong environmental covariance. Cellular trait based models use detailed studies of phytoplankton physiology to determine how phytoplankton cells should allocate their resources as a functional of environmental conditions, allowing us to model the interactive influence of temperature, nutrient concentrations, and irradiance on C:P ratios (Clark et al., 2011; Daines et al., 2014; Shuter, 1979; Talmy et al., 2014; Toseland et al., 2013). Numerous physiological mechanisms have been proposed to explain variation in phytoplankton stoichiometry, including growth rate (Sterner and Elser, 2002), photoacclimation (Falkowski and LaRoche, 1991; Geider et al., 1996; Leonardos and



Geider, 2004, 2005), nutrient-limitation responses (Garcia et al., 2016; Goldman et al., 1979; Rhee, 1978), and temperature acclimation (Rhee and Gotham, 1981; Toseland et al., 2013; Yvon-Durocher et al., 2015). Through incorporation of such physiological responses, a trait-based model has revealed that differences in ribosomal content and cell radius between warm-water, oligotrophic environments and cold-water, eutrophic environments are important mechanisms driving stoichiometric variation in the ocean (Daines et al., 2014). Thus, linking biome-scale variations in environmental conditions with a detailed trait-based model of phytoplankton resource allocation and elemental composition may enable us to more fully explore interactions among ocean environmental conditions, the biological pump, and $p\text{CO}_{2,\text{atm}}$.

Here we create a five-box model, incorporating the three major ocean biomes, to study the feedback effects of variable stoichiometry on carbon export and $p\text{CO}_{2,\text{atm}}$. We will explicitly address the following research questions: (1) How does environmental variability influence marine phytoplankton stoichiometry? (2) What are the effects of changing environmental conditions on stoichiometric ratios, carbon export, and $p\text{CO}_{2,\text{atm}}$?, and (3) What is the influence of the environmental gradients among the three major surface biomes on carbon export and $p\text{CO}_{2,\text{atm}}$?

2 Methods

2.1 Stoichiometric Models

To quantify and understand the feedbacks between carbon export and $p\text{CO}_{2,\text{atm}}$, we embedded four stoichiometric models into our box model. We included four distinct stoichiometric models to calculate $\text{C:P}_{\text{export}}$, each of which differs according to their complexity and how much environmental information they utilize. These are a static Redfield model that assumes that $\text{C:P}_{\text{export}}$ is a constant function of environmental conditions, a nutrient-only model that uses surface $[\text{P}]$ to predict $\text{C:P}_{\text{export}}$ (from Galbraith and Martiny, 2015), a temperature-only model that uses T to predict $\text{C:P}_{\text{export}}$ (modified from Yvon-Durocher et al., 2015), and a multi-environmental model that uses light, T , and $[\text{P}]$ to predict $\text{C:P}_{\text{export}}$.

2.1.1 Static Redfield Model

Our control model uses a static Redfield stoichiometry. The Redfield ratio is based on an average value of organic carbon to phosphorus of 106:1.

2.1.2 Nutrient-Only Model

The nutrient-only stoichiometric model expresses phytoplankton C:P as a function of the ambient phosphate concentration:

$$\text{C:P} = \frac{1}{\kappa[\text{P}] + [\text{P}]_0}, \quad (1)$$

where the parameters $\kappa = 6.0\mu\text{M}^{-1}$ and $[\text{P}]_0 = 6.9$ were obtained by regressing the reciprocal of C:P onto $[\text{P}]$ (Galbraith and Martiny, 2015).

2.1.3 Temperature-Only Model



The temperature-only stoichiometric model expresses phytoplankton C:P as a function of temperature:

$$\ln(\text{C:P}) = \Pi(T - 15^\circ\text{C}) + b, \quad (2)$$

where the parameters $\Pi = 0.037/^\circ\text{C}$ and $b = 5.5938$ (Yvon-Durocher et al., 2015). The temperature-only model was created to determine the temperature responses of log-transformed C:P ratios centered at 15°C .

2.1.4 Multi-Environmental Model

The multi-environmental factor model was derived from a non-dynamic physiological trait-based model. We used a theoretical cellular-allocation trait model based on phytoplankton physiological properties that divides the 'cell' into functional pools including ribosomes, proteins, the cell membrane, and storage molecules. Storage pools include carbohydrates, lipids, and P containing molecules such as polyphosphates and phospholipids. The model predicts the size of each pool as a function of light, T , and $[P]$. The size of each functional pool is modeled by using subcellular resource compartments, which connect the fitness of a hypothetical phytoplankton cell in a given environment to its cellular radius and the relative allocation of cellular material to photosynthetic proteins, ribosomes, and biosynthetic proteins. We assume that real phytoplankton populations have physiological behaviors that cluster around the strategy that produces the fastest growth rate in each environment (Norberg et al., 2001), and use the stoichiometry of this optimal strategy to model the elemental composition of cellular material (Figure 1).

Phytoplankton can accumulate large reserves of nutrients that are not immediately incorporated into the functional components of the cell (Diaz et al., 2016; Mino et al., 1998; Van Mooy and Devol, 2008; Mouginot et al., 2015). This storage capability varies among phytoplankton species, and depends on the particular nutrient under consideration: the cost for storing physiologically relevant quantities of nutrients is low for nutrients with low quotas such as phosphorus, in comparison to nitrogen and carbon. Thus, the phosphorus storage is assumed highly plastic in comparison to carbon storage (Moore et al., 2013). Further, we assume that each cell dedicates a fixed fraction of its biomass to carbon reserves, and focus our modeling efforts on the variability of the stored phosphorus pool. To predict the size of the storage pool, we assume a linear relationship between stored phosphorus and ambient environmental phosphorus levels and used statistical modeling of an oceanic C:P dataset (Martiny et al., 2014) to calculate the constant of proportionality. The result is a relatively simple model that both qualitatively and quantitatively predicts the variation of C:P in plankton throughout the oceans.

Phytoplankton physiology is modeled through allocations of cell dry mass to three distinct pools: structure ($S(r)$), biosynthesis (E), and photosynthesis (L). Allocations satisfy:

$$1 = S(r) + E + L, \quad (3)$$

where the variables S , E , and L represent the *specific* allocations of cellular biomass.

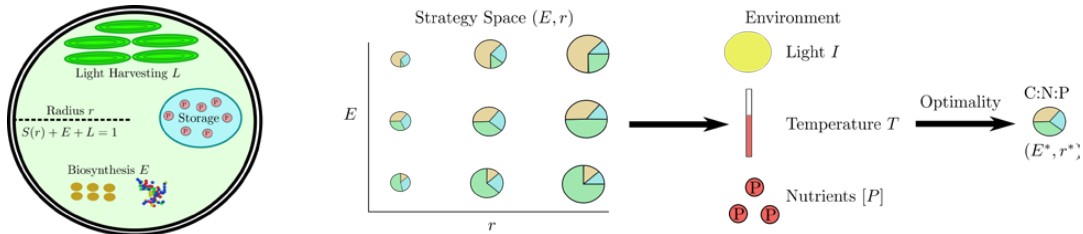


Figure 1: Diagram of physiological model. Phytoplankton strategies are represented in a two-dimensional strategy space (E, r) . Each strategy is assigned a fitness in each environment using physiological principles, and the strategy with the highest fitness is selected to represent the local population. The stoichiometry of cellular components is used to calculate the stoichiometry of the functional pools in the cell.

The specific allocation of biomass to the cell membrane is inversely proportional to the cell radius (α/r) (Clark et al., 2011), which accounts for the changing relative volume of the cell-membrane with radius. The structure pool includes the cell membrane plus wall and other components (γ), which are not related to photosynthesis or biosynthesis and is given by:

$$S(r) = \frac{\alpha}{r} + \gamma. \quad (4)$$

In an environment specified by T , $[P]$, and light level (I), the growth rate of a cell using a given strategy is the minimum of the following growth rates:

$$\mu = \min(\mu_E, \mu_L, \mu_P). \quad (5)$$

Here μ_E is determined by the specific rate of protein synthesis, μ_L is determined by the specific rate of carbon fixation, and μ_P is determined by the specific rate of phosphorus uptake, or:

$$\mu_E = k_E(T)E, \quad \mu_L = \frac{f_P(L, I) - \Phi_M(T)}{1 + \Phi_S}, \quad \mu_P = \frac{1}{Q_P(r, E)} \frac{V_m(r)[P]}{K_P(r) + [P]}. \quad (6)$$

We assume that part of the energy captured by a cell via photosynthesis is used for maintenance (Φ_M), whereas the rest is used to drive the synthesis of new macromolecules (Φ_S), so that a cell growing at rate μ_L is in energy balance. The efficiency of biosynthesis k_E and the carbon cost of maintenance Φ_M are functions of T , whose dependence is modeled using $Q_{10} = 2.0$ (Van Bogelen and Neidhardt, 1990; Broeze et al., 1978; Shuter, 1979). Uptake is regulated by a Monod function with kinetic parameters depending on the radius through the allometric scaling relationships derived from measurements of phytoplankton populations (Edwards et al., 2012):

$$V_m(r) = a_P r^{b_P}, \quad K_P(r) = a_K r^{b_K}. \quad (7)$$

This use of allometric scaling relationships departs from the conventions adopted by Shuter (1979) or Daines (2014), who assume that uptake rates are diffusion-limited.



The phosphorus quota for functional elements of the cell is determined by the allocation to biosynthesis E and the percentage p_{DNA} of cellular dry mass allocated to DNA:

$$Q_p(E, r) = \frac{4}{3} \pi r^3 \rho_{\text{cell}} p_{\text{dry}} \frac{(\alpha_E E P_{\text{rib}} + p_{\text{DNA}} P_{\text{DNA}})}{31}. \quad (8)$$

Here we assume that there is no contribution to the functional-apparatus P quota from phospholipids, which instead is merged with storage molecules. This differs from Daines (2014), who assume that phospholipids occupy 10% of the cell by mass. Phytoplankton can substitute sulfoquinovosdiacylglycerol (SQDG) for phospholipids in their cell membranes in low P conditions (Van Mooy et al., 2006), implying that it is appropriate to functionally treat them together with the storage pool.

The function f_p is the response of the cell to light levels, and is chosen to capture the effects of both electron transport and carbon fixation on photosynthesis (Talmy et al., 2014). Our model interprets the light harvesting allocation L as being composed of proteins dedicated to carbon fixation (F_1), such as RuBisCO, and proteins dedicated to electron transport (F_2), such as photosynthetic pigments. The rate of photosynthetic carbon fixation is a function of the allocations to each of these, which satisfy $F_1 + F_2 = L$. The relative allocations together determine the overall photosynthetic rate:

$$P_{\text{max}} = \min(k_1 F_1, k_2 F_2), \quad f_p = P_{\text{max}} \left(1 - \exp \left(\frac{-\alpha_{\text{ph}} \phi_M F_2 I}{P_{\text{max}}} \right) \right). \quad (9)$$

For a given I and L , there is a pair of values $(F_{1,\text{opt}}, F_{2,\text{opt}})$ that maximize the photosynthetic rate f_p . We estimate the photosynthetic rate $f_p(L, I)$ under the assumption that cells assume the optimal allocations to carbon fixation and electron transport. This model departs from the models developed by Shuter (1979) and Daines (2014), which assume that energy acquisition is a linear function of light levels, with functional response linearly proportional to the cellular investment in light harvesting proteins.

We assume that real phytoplankton populations cluster near the optimal strategy in the local environment (Norberg et al., 2001):

$$(E_m, r_m) = \text{argmax}_{(E, r)} \mu. \quad (10)$$

For all values of environmental parameters used in this study, the unique maximum of the growth rate occurs for the set of parameter values that lead to co-limitation by nutrients, photosynthesis, and biosynthesis, analogously to the predictions of Klausmeier et al. (2004). The optimal strategy determines the model prediction of the C:P of functional components in a given environment by taking the quotient of the carbon and phosphorus quotas.

Table 1. Physiological Model Constants.

PARAMETER	DESCRIPTION	VALUE	UNITS	SOURCE
α	Proportionality coefficient for radius	0.12	-	(Toseland et al., 2013)
γ	Percent dry mass devoted to structure	0.2	-	(Toseland et al., 2013)



	other than membrane			
k_{E0}	Synthesis rate of biosynthesis apparatus at $T_0=25$	0.168	hr^{-1}	(Shuter, 1979)
$Q_{10,E}$	Q_{10} of biosynthetic apparatus	2.0		(Shuter, 1979)
Φ_{M0}	Specific carbon cost of maintenance at $T_0=25$	10^{-3}	hr^{-1}	(Shuter, 1979)
$Q_{10,M}$	Q_{10} of maintenance	2.0	-	(Shuter, 1979)
Φ_S	Carbon cost of synthesis	0.67	-	(Shuter, 1979)
a_P	Allometric scaling constant for V_{MP}	1.04×10^{-16}	$(\text{mol P})(\text{hr})^{-1}$	(Edwards et al., 2012)
b_P	Allometric scaling exponent for V_{MP}	3.0	-	(Edwards et al., 2012)
a_K	Allometric scaling constant for K_P	6.4×10^{-8}	$(\text{mol P})(\text{L})^{-1}$	(Edwards et al., 2012)
b_K	Allometric scaling exponent for K_P	1.23	-	(Edwards et al., 2012)
ρ_{cell}	Cell Density	10^6	g/m^3	(Shuter, 1979)
p_{dry}	Fraction of dry mass in cell	0.47	-	(Toseland et al., 2013)
α_E	Fraction of dry mass in biosynthetic apparatus devoted to ribosomes	0.55	-	(Toseland et al., 2013)
P_{rib}	Fraction of ribosomal mass in phosphorus	0.047	-	(Sternner and Elser, 2002)
p_{DNA}	Fraction of cell dry mass in DNA	0.01	-	(Toseland et al., 2013)
P_{DNA}	Fraction of DNA mass in phosphorus	0.095	-	(Sternner and Elser, 2002)
k_1	Specific Efficiency of Carbon Fixation Apparatus	0.373	hr^{-1}	(Talmy et al., 2013)
k_2	Specific Efficiency of Electron Transport Apparatus	0.857	hr^{-1}	(Talmy et al., 2013)
α_{Ph}	Light Absorption	1.97	m^2/gC	(Morel and Bricaud, 1981)
Φ_M	Maximum Quantum Efficiency	10^{-6}	$\text{gC}/\mu\text{mol photons}$	(Falkowski and Raven, 1997)
m_{lip}	Fraction of cell membrane composed of lipids	0.3	-	(Toseland et al., 2013)
m_{prot}	Fraction of cell membrane composed of protein	0.7	-	(Toseland et al., 2013)
p_{lip}	Fraction of cell dry mass in storage lipids	0.1	-	(Sternner and Elser, 2002)
p_{carb}	Fraction of cell dry mass in storage	0.04	-	(Sternner and Elser, 2002)



	carbohydrates			
C_{DNA}	Fraction of DNA mass in Carbon	0.36	-	(Sterner and Elser, 2002)
C_{rib}	Fraction of ribosomal mass in Carbon	0.42	-	(Sterner and Elser, 2002)
C_{prot}	Fraction of protein mass in Carbon	0.53	-	(Sterner and Elser, 2002)
C_{lip}	Fraction of lipid mass in Carbon	0.76	-	(Sterner and Elser, 2002)
C_{carb}	Fraction of carbohydrate mass in Carbon	0.4	-	(Sterner and Elser, 2002)

The carbon quota is calculated as:

$$Q_C = \frac{4}{3} \pi r^3 \rho_{cell} p_{dry} \frac{\left(\alpha_E E C_{rib} + \left((1 - \alpha_E) E + L + \frac{m_{prot} \alpha}{r} \right) C_{prot} + p_{DNA} C_{DNA} + \left(\frac{m_{lip} \alpha}{r} p_{lip} \right) C_{lip} + p_{carb} C_{carb} \right)}{12} \quad (11)$$

Here we see the contributions of carbon contained in both functional and storage pools, the latter of which are assumed to occupy a fixed fraction of the cell independent of the environment.

245 Measurements of cellular P partitioning indicate that the ribosomal RNA can sometimes contribute only 33% of the total P quota (Garcia et al., 2016). The additional phosphorus includes membrane phospholipids, luxury storage compounds, and polyphosphates, each of which can be up- or down-regulated in response to phosphorus availability in the environment. To model this phenomenon, we assume the existence of an
 250 additional stored P pool, whose size is a linear function of environmental P, or:

$$(P:C)_{storage} = \epsilon [P], \quad (12)$$

where ϵ is determined by the best fit to the Martiny et al. (2014) data. Our model then predicts C:P as:

$$C:P = \frac{1}{(P:C)_{(E_m, r_m)} + \epsilon [P]} \quad (13)$$

255 The model parameter ϵ is calculated by minimizing the residuals of the P:C ratio predicted by Eq.13 in comparison to the global data-set on particulate organic matter stoichiometry compiled by Martiny and others (2014). To maintain consistency with the linear regression model of Galbraith and Martiny (2015), we restrict the dataset to observations from the upper 30 meters of the water column containing particulate organic phosphorus and carbon concentrations of greater than $0.005 \mu M$. Observations from the same station and
 260 the same day, but at different depths in the water column are averaged together. The P:C ratio of the functional apparatus is calculated using T , $[P]$, and irradiance data from the World Ocean Atlas (Garcia et al., 2014; Locarnini et al., 2013; oceancolor.gsfc.nasa.gov/data/10.5067/AQUA/MODIS/L3B/PAR/2014/), which are used to estimate environmental conditions at the location and date of particulate organic matter
 265 measurements. Light levels are computed by averaging irradiance over the top 50 meters



of the water column, assuming an e-folding depth of 20 meters. Linear regression determines $\epsilon = 2500 \text{ M}^{-1}$ which fits the data with an $R^2 = 0.28$. All parameters for the model are listed in Table 1.

2.2 Box Model Design

To quantify the feedbacks between phytoplankton stoichiometry, carbon export, and $\text{pCO}_{2,\text{atm}}$, we formulated a five-box model of the phosphorus and carbon cycles in the ocean and atmosphere. The foundation of our model is based on the models introduced in Ito and Follows (2003) and DeVries and Primeau (2009). The model includes three surface boxes, each corresponding to one of the major biomes: the tropical equatorial upwelling regions (labeled T), the subtropical gyres (labeled S), and the high-latitude regions (labeled H) (Figure 2). We define the oligotrophic subtropical gyre regions where the mean annual phosphate concentration is less than $0.3 \mu\text{M}$ (Teng et al., 2014), with the remainder of the surface ocean assigned either to box T or box H based on latitude. We use these assignments to calculate the baseline physical properties of each region, including mean annual averaged irradiance and temperature. The subsurface ocean is divided into two regions: the thermocline waters that underlies the subtropical gyres, the equatorial upwelling regions (labeled M), and deep waters (labeled D) (DeVries and Primeau, 2009).

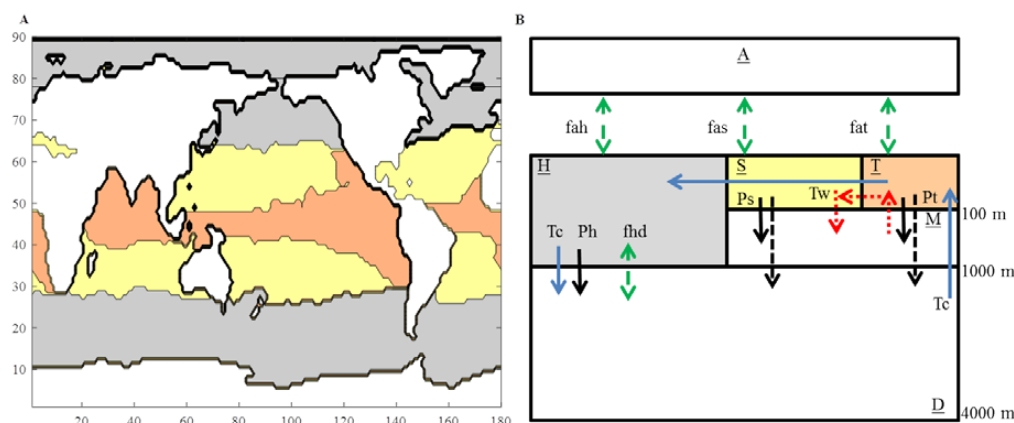


Figure 2: Box Model Design. A) Sea surface breakdown by region. All regions peach color represents the tropical surface ocean box, cream represents the subtropical surface ocean box, and grey color represents the high-latitude surface ocean box. B) The model includes tropical (T), subtropical (S), and high-latitude (H) surface ocean boxes, a mixed thermocline (M) box, and a deep water (D) box. The thermohaline circulation T_c is set to 20 Sv, while the wind driven shallow overturning circulation is set to 5 Sv. The high-latitude mixing flux f_{hd} is set to 45.6 Sv. The thickness of Box H is 1000 m, and Box M is 900 m. Box T has a T of 26°C , box S has a T of 24°C , and box H has a T of 7°C . Box S covers 39% and Box T covers 25% of the ocean surface area.

To simulate the global transport of water between boxes, our model includes a thermohaline circulation (labeled T_c) that upwells water from the deep ocean into the tropics, laterally transports water into the subtropics and high-latitudes, and downwells water from the high-latitude region to the deep ocean. Surface winds produce a shallow overturning circulation (labeled T_w), that transports water from the thermocline to the tropics and then laterally into the subtropics. These circulations create teleconnections of



300 nutrient supply in the surface ocean boxes. A bidirectional mixing term that ventilates the
deep box directly through the high-latitude surface box (labeled fhd) represents deep
water formation in the Northern Atlantic region and around Antarctica (Sarmiento and
Toggweiler, 1984). The parameters T_c , T_w and fhd are considered adjustable parameters,
which we calibrate using phosphate data from WOA13 (Garcia et al., 2014). In order to
305 simulate the movement of particles, we included export fluxes (P_t , P_s , and P_h) of organic
phosphorus out of each surface box.

Our box model simulates [P], alkalinity and various forms of C; total carbon in the
surface boxes is partitioned into carbonate, bicarbonate, and pCO_2 . The global mean [P] is
prescribed according to the observed mean ocean value (Garcia et al., 2014). The export of
carbon is linked to phosphorus export using the $C:P_{export}$ ratio. To quantify the breakdown
310 of carbon into these components, we model the solubility pump, using temperature and
salinity to determine the partitioning of inorganic carbon. CO_2 cycles through the
atmosphere via the air-sea gas exchange fluxes (f_{ah} , f_{as} , f_{at}). We used a uniform piston
velocity of $5.5 \times 10^{-5} \text{ m s}^{-1}$ to drive air-sea gas exchange (DeVries and Primeau, 2009;
Follows et al., 2002). Iron limitation is implicitly simulated through its control on the
315 tropical [P], which is used as a control variable in our experimental runs.

We calibrated our model parameters (T_c , T_w , fhd) so that the macronutrients were
at similar average values based on the World Ocean Atlas 2013 dataset for its location. We
tested the sensitivity of modeled $pCO_{2,atm}$ to the fluxes T_c , T_w , and fhd and found that with
 $T_c = 20 \text{ Sv}$ and $T_w = 5 \text{ Sv}$ (values that allowed the model to match [P] and alkalinity) the
320 $pCO_{2,atm}$ was sensitive to the value of fhd (Sarmiento and Toggweiler, 1984). Guided by
values previously used in the literature we set fhd to 45.6 Sv (Table 2) but we also present
results for the nutrient-only stoichiometry model at two extreme values of fhd, 18 and 108
Sv (Figure 3). The functional dependence of $pCO_{2,atm}$ with changing subtropical and tropical
[P] for each extreme value of fhd was quite similar, though the value of $pCO_{2,atm}$ for the high
325 fhd simulation was approximately twice that of the low fhd simulation (Figure 3). We found
that our value of 45.6 Sv provides a modern $pCO_{2,atm}$ value.

For certain values of the parameters, the model produced excessive nutrient
trapping in the thermocline. In order to dampen the nutrient trapping, we tuned the
remineralization depth. Assuming that 25% of the total export is respired in the
330 thermocline with the remaining 75% exported into the deep ocean, produced a better
match between the modeled and observed [P] in the thermocline box.

Table 2: High-latitude deep water exchange range

REFERENCE	RANGE OF FHD [SV]
Sarmiento and Toggweiler, 1984	38.1
Toggweiler, 1999	3-300
Devries and Primeau, 2009	60
Galbraith and Martiny, 2015	30-130
This Study	18-108 (default value 45.6)

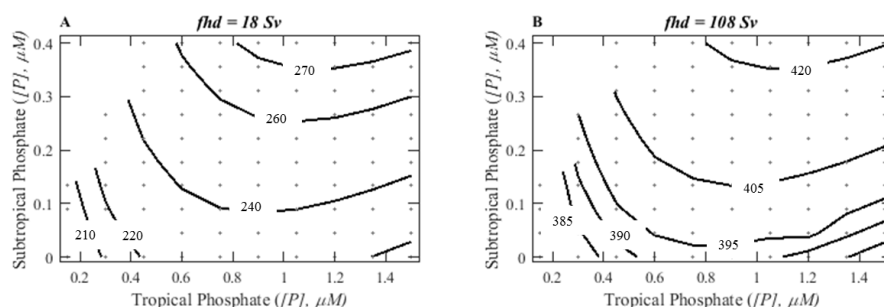


Figure 3: $p\text{CO}_{2,\text{atm}}$ (ppm) sensitivity to extreme fhd values under changing surface phosphate concentrations. A.) Range of $p\text{CO}_{2,\text{atm}}$ (ppm) using an fhd value of 18 Sv. B.) Range of $p\text{CO}_{2,\text{atm}}$ (ppm) using an fhd value of 108 Sv.

2.2.1 Experimental Design

To address how changing environmental conditions affected stoichiometric ratios, carbon export, and $p\text{CO}_{2,\text{atm}}$ we performed two tests; a change in nutrients and a change in sea surface temperature. These tests allowed us to observe how the relationships between environmental conditions, carbon export and $p\text{CO}_{2,\text{atm}}$, depend on the mechanisms responsible for stoichiometric variation in the ocean. In order to account for the effects of particulate inorganic carbon (PIC) export, we multiply model predicted $\text{C:P}_{\text{export}}$ by 1.2, consistent with previous studies (Broecker, 1982; Sarmiento and Toggweiler, 1984).

The first set of numerical experiments examined the sensitivity of $p\text{CO}_{2,\text{atm}}$ to nutrient availability in the tropical and subtropical boxes for each of the three stoichiometric models. This set of experimental runs was intended to capture the effects of changing levels of iron deposition, which could lead to shifts in phosphorus drawdown by relieving iron limitation of diazotrophic phytoplankton in subtropical gyres and of bulk phytoplankton populations in equatorial upwelling regions. We varied tropical $[\text{P}]$ from 0.15 to 1.5 μM and subtropical $[\text{P}]$ from 0 to 0.5 μM by adjusting the implied biological export and determined the equilibrium $p\text{CO}_{2,\text{atm}}$ values.

The second set of experimental tests was done to quantify how temperature modifies carbon export and $p\text{CO}_{2,\text{atm}}$ for each stoichiometric model. Temperature influences carbon cycling in two ways within our model: through the solubility of inorganic carbon in seawater and through changes in phytoplankton stoichiometry within the temperature-only and multi-environmental models. Due to the well-known effects of temperature on CO_2 solubility, it is generally predicted that there is to be a positive feedback between $p\text{CO}_{2,\text{atm}}$ and temperature mediated by declining CO_2 solubility at high T 's. To study the relative strengths of the temperature solubility feedback and the temperature regulation of C:P feedback, we performed a numerical experiment in which we varied the sea surface temperature by five degrees in either direction of modern sea surface temperature. This represents a plausible range of variation under both ice-age and anthropogenic climate change scenarios. We varied tropical temperature from 21° to 31°C and subtropical temperature from 19° to 29°C, determining equilibrium $p\text{CO}_{2,\text{atm}}$ values for combinations of temperature conditions.



3 Results

To quantify the linkages between phytoplankton physiology, elemental stoichiometry, and ocean carbon cycling, we divide our results into two parts. The first is a direct study of the stoichiometric models, comparing their predictions about the relationship between stoichiometry and environmental conditions, and in the case of the trait-based model, illustrating how cellular physiology is predicted to vary across these conditions. In the second part, we show how variables stoichiometry influences carbon export and $p\text{CO}_{2,\text{atm}}$, under changing phosphorus concentrations and temperature. Within these results, we distinguish the influence or lack thereof on the three distinct biomes, in particular the iron stressed equatorial upwelling regions and the macronutrient depleted subtropical gyres.

3.1 Multi-environmental and physiological controls on plankton stoichiometry

Our multi-environmental model captured several major mechanisms hypothesized to be environmental drivers of C:P ratios including a temperature dependence of many cellular processes, a link between growth rate and ribosome abundance, and storage drawdown during nutrient limitation. The predicted relationship between environmental conditions and C:P can be understood through the environmental regulation of three factors: (i) the balance between photosynthetic proteins and ribosomes, (ii) the cell radius and associated allocation to structural material, and (iii) the degree of phosphorus storage. Our model predicted that for an optimal strategy, specific protein synthesis rates will match specific rates of carbon fixation. Thus, the ratio of photosynthetic machinery to biosynthetic machinery is therefore primarily controlled by irradiance and temperature. Increases in light levels lead to higher photosynthetic efficiency, higher ribosome content, and lower C:P ratios (Figure 4). The response of C:P to light levels predicted by our model was muted in comparison to other subcellular compartment models because we separately modeled electron transport and carbon fixation (Talmy et al., 2014), and our predictions were consistent with the weak relationship between irradiance and C:P (Thrane et al., 2016) (Figure 4A). Increases in temperature increase the efficiency of biosynthesis, but not photosynthesis. Therefore elevated temperature lead to a reduced ribosome content relative to photosynthetic proteins and higher C:P ratios (Figure 5A). Nutrient concentrations do not affect the ratio of biosynthetic to photosynthetic machinery but positively relate to both P storage and cell radius. Cell radius directly influences the specific rate of nutrient uptake, and indirectly biosynthesis and photosynthesis as the cell membrane and wall affects the space available for other investments. This effect becomes pronounced at small radius. In oligotrophic conditions ($[\text{P}] < 100\text{nM}$), cell radius declines substantially, decreasing the allocations to both photosynthesis and biosynthesis and driving up C:P ratios. P concentrations also influenced C:P through their direct control of P storage. Thus, C:P was predicted to be a decreasing function of $[\text{P}]$ with two distinct regimes: a moderate sensitivity regime for $[\text{P}]$ above 100nM , and a high sensitivity regime for $[\text{P}]$ below 100nM .

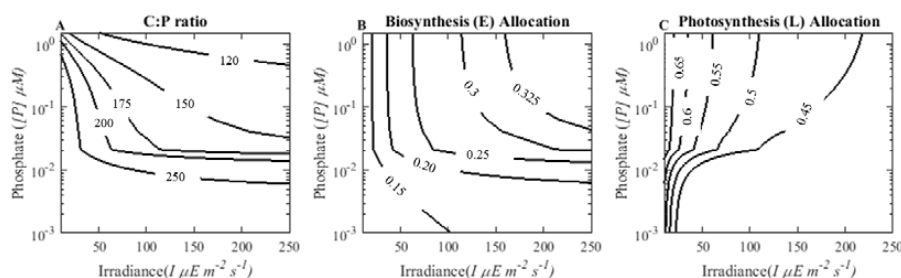


Figure 4: Influence of phosphate concentration and irradiance on cellular stoichiometry and cellular traits, at a constant $T = 25\text{ °C}$. A) The C:P ratio. B) Biosynthesis allocation. C) Photosynthesis (L) allocation. As irradiance increases, there is a tendency towards greater allocation to biosynthesis and lesser allocation to photosynthesis, which leads to lower C:P ratios. When phosphorus is very low, there is a large decrease in both biosynthesis and photosynthesis allocations due to the large relative allocation to the cell membrane. C:P ratios are inversely proportional to phosphorus concentration, driven by an increase in luxury storage and ribosomal content as P increases.

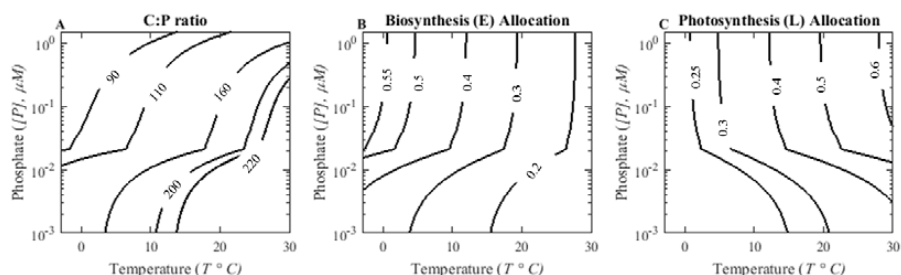


Figure 5: Influence of phosphate concentration and temperature on cellular stoichiometry and cellular traits, at a constant irradiance $I = 50\text{ μE m}^{-2}\text{ s}^{-1}$. A) The C:P ratio. B) Biosynthesis allocation. C) Photosynthesis (L) allocation. Consistent with the translation compensation hypothesis, increases in T led to a reduction in the allocation to biosynthesis and an increase in C:P.

We next used the outcome of the trait model as a multi-environmental model to predict C:P ratios in the modern ocean based on annual mean light, T , and $[P]$. Our predictions reproduced the global pattern (Martiny et al., 2014) with C:P ratios above the Redfield ratio in subtropical gyres and C:P ratios below the Redfield ratio in equatorial and coastal upwelling regions and subpolar gyres (Figure 6A). Additionally, our model also reproduced basin-scale stoichiometric gradients among similar biomes in each ocean, predicting the highest C:P ratios in the western Mediterranean Sea and the western North Atlantic Subtropical Gyre, and somewhat elevated C:P ratios in the South Atlantic Subtropical Gyre as well as the North and South Pacific Subtropical Gyres.

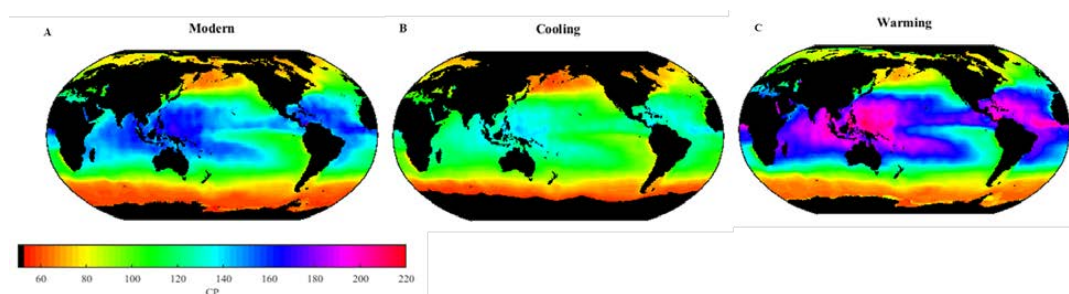


Figure 6: Predicted C:P ratios in the global ocean in differing climatic regimes. A) C:P ratio under modern ocean conditions. Large differences in C:P are predicted between distinct types of ocean biome, with low C:P in equatorial upwelling regions and subpolar gyres, and high C:P in subtropical gyres. Regional differences between biomes of similar type are observed as well, with the low phosphorus Atlantic having a higher C:P than the Pacific. B.) C:P ratio under cooling temperature conditions (-5°C from the modern ocean). C) C:P ratio under warming temperature conditions ($+5^{\circ}\text{C}$ from the modern ocean). Each 5 degree change leads to a shift of 15% in the mean C:P ratio of organic matter.

To study the potential impact of sea surface temperature on phytoplankton resource allocation and stoichiometry, we used our multi-environmental model to predict C:P in ocean conditions both five degrees colder (Cooling environments) and warmer (Warming environments) than the modern ocean. According to our model, a five-degree increase (or decrease) in sea surface temperature would cause a 15% rise (or fall) in C:P ratios (Figure 6). This sensitivity suggested that the relative effect of T on biochemical processes could have large implications for biogeochemical cycles, making it important to determine the relative importance of physiological mechanisms regulating C:P ratios.

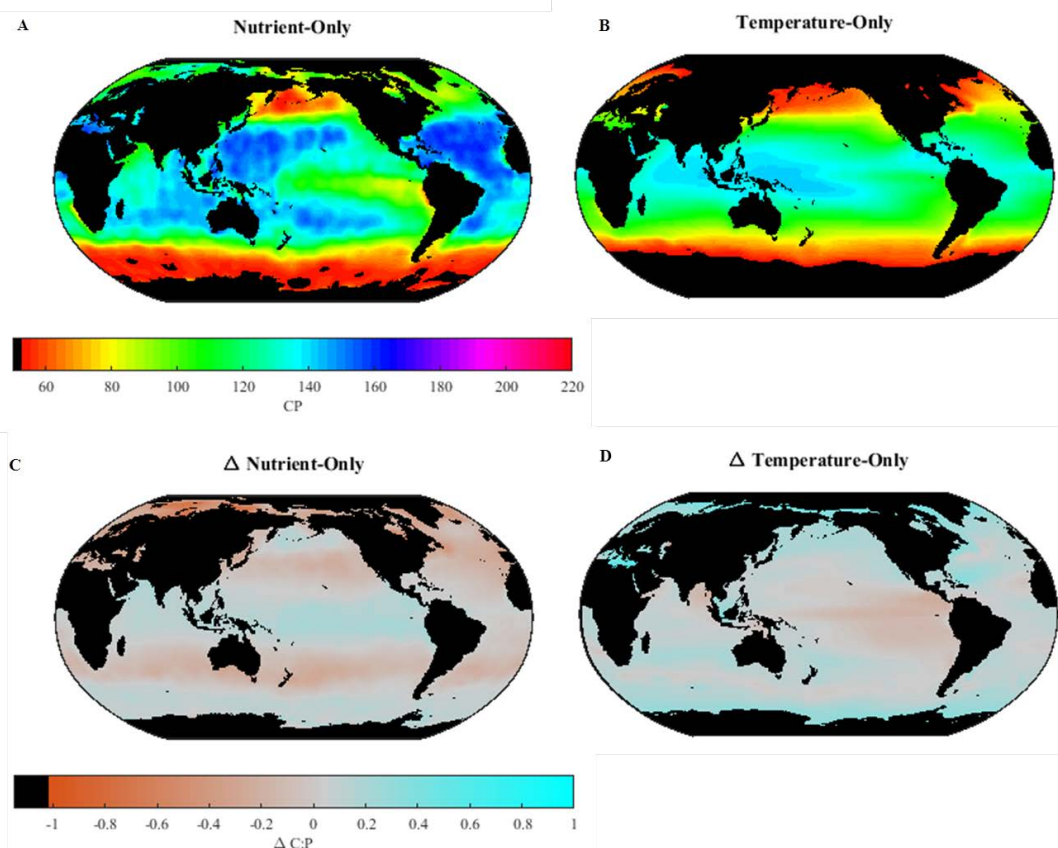


Figure 7: Comparison of C:P between the multi-environmental model and the nutrient-only model and temperature-only model. The upper panels show predicted C:P for the global ocean under the nutrient-only (A) and temperature-only (B) models, and the lower panels show the normalized difference, i. e. $\frac{C:P_{subcell} - C:P_{other}}{C:P_{subcell}}$, between the C:P in the subcellular model (C, D).

We compared the multi-environmental model to the predictions made by two other models: the nutrient-only model used by the Galbraith and Martiny model (2015), and our temperature-only model modified from Yvon-Durocher and co-workers (2015). These two models also successfully predicted the qualitative pattern of stoichiometric variation in the ocean, but were unable to replicate the full range of variation observed in data (Figure 7). In particular, they misrepresented the North Atlantic Subtropical Gyre and the Southern Ocean, where the C:P ratio is at the extreme (Figure 7A, B). The nutrient-only model had a tendency to predict lower C:P ratios than the multi-environmental model in warm tropical and subtropical waters, and predict higher C:P ratios in cold waters (Figure 7A). This difference is driven by the T sensitivity of biosynthesis in the multi-environmental model, leading to increasing C:P in all warm water regions and decreasing C:P in cold water regions (Figure 7C). The multi-environmental model predicted a wider range of C:P in the ocean. The temperature-only model overall had higher C:P ratios globally compared with



the multi-environmental model (Figure 7B) but suggested lower C:P in the gyres and higher C:P in high latitudes, especially in the Southern Ocean (Figure 7D).

3.2 Impact of nutrient availability on carbon export and atmospheric $p\text{CO}_2$

480 We next quantified the impact of nutrient availability in the tropics and subtropics on stoichiometry, carbon export and $p\text{CO}_{2,\text{atm}}$ (Figure 8A-L). Using a constant Redfield model (or the temperature-only model), we replicated the previously observed approximately linear relationship between surface [P] and $p\text{CO}_{2,\text{atm}}$ (equivalent to how pre-formed [P] will influence $p\text{CO}_{2,\text{atm}}$) (Ito and Follows, 2003; Sigman and Boyle, 2000). We found that [P] drawdown in the subtropical box had a greater impact on carbon export, since export from the high-latitude box was not enhanced by the [P] supply from the subtropical box (Figure 8A, D, G). In the Redfield model, $p\text{CO}_{2,\text{atm}}$ appeared to be much more sensitive to subtropical [P] than tropical [P], which was partially due to enhanced carbon export in the subtropical box and partially due to the larger surface area of the subtropical box (implying a greater potential for CO_2 exchange) (Figure 8J).

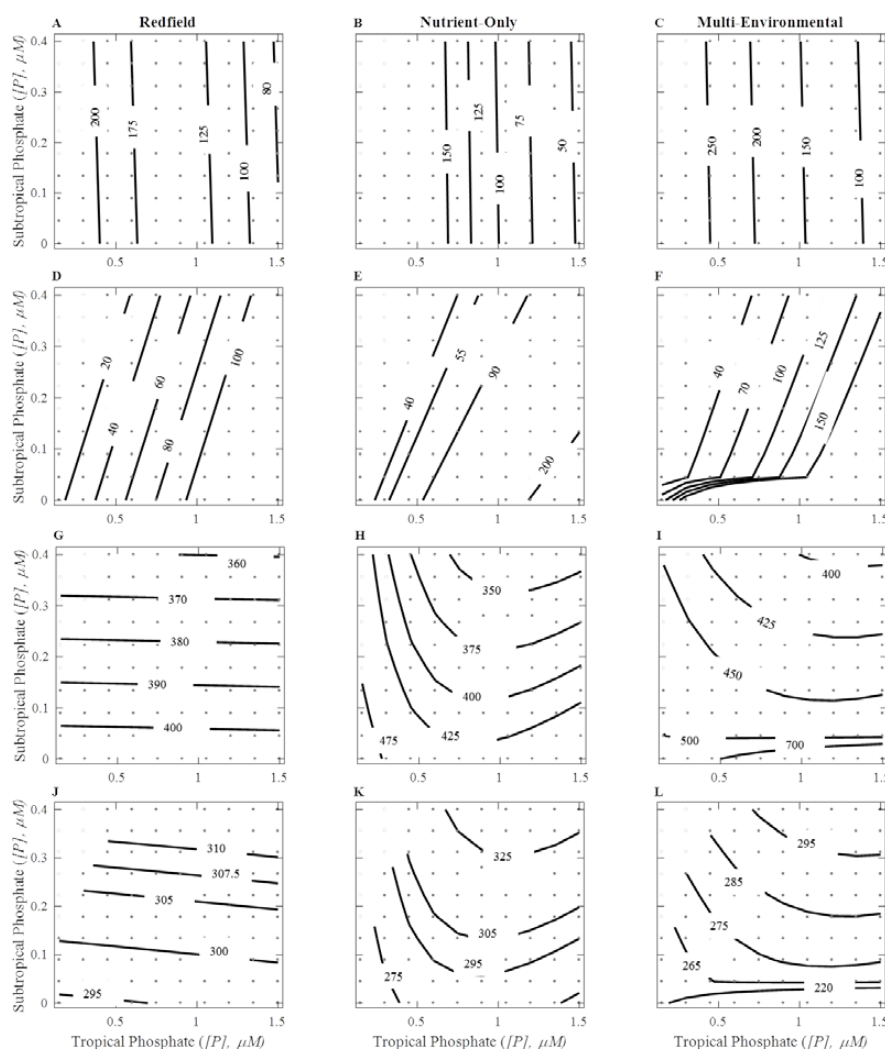
485 In contrast to the predictions made using Redfield stoichiometry, when we used the nutrient-only model for phytoplankton stoichiometry, we observed a non-linear relationship between surface [P] and $p\text{CO}_{2,\text{atm}}$ (Figure 8B, E, H, K). At fixed tropical [P], there was a strong relationship between subtropical [P], export, and $p\text{CO}_{2,\text{atm}}$ in accordance with the findings of Galbraith and Martiny (2015) (Figure 8B, E, H). The total decline in $p\text{CO}_{2,\text{atm}}$ as subtropical [P] declined from 0.4 μM to 0 μM could be more than 60 ppm, which was more than twice the decline that occurred in the fixed stoichiometry experiment (Figure 8K). We found a non-linear monotonic relationship between tropical [P] and $p\text{CO}_{2,\text{atm}}$: when tropical [P] was high, declines in tropical [P] led to lower carbon export and increased $p\text{CO}_{2,\text{atm}}$. However, this trend reversed when tropical [P] was lower (Figure 8K). The counter intuitive decline in $p\text{CO}_{2,\text{atm}}$ with higher export from tropics was driven by a teleconnection in nutrient delivery between the subtropical and tropical boxes. Increases in export in the tropical box due to increased [P] drawdown decreased the supply of [P] to the subtropics, which led to a decrease in the more efficient (higher C:P) subtropical export. 495 Thus, the nutrient-only model predicted a greater decrease in subtropical export than the counter increase in tropical export.

500 The multi-environmental model also predicted a non-linear relationship between surface P, carbon export, and $p\text{CO}_{2,\text{atm}}$. However, the pattern was somewhat distinct from that of the nutrient-only model results (Figure 8C, F, I, L). First, subtropical [P] drawdown had a nonlinear relationship with $p\text{CO}_{2,\text{atm}}$: when subtropical [P] was high, declines in subtropical [P] led to slight declines in $p\text{CO}_{2,\text{atm}}$, and when subtropical [P] is low, small declines in tropical [P] lead to large declines in $p\text{CO}_{2,\text{atm}}$. This intensification of the relationship between subtropical [P] and $p\text{CO}_{2,\text{atm}}$ was due to the nonlinear relationship between [P] and C:P predicted by the trait-based model (Figure 8I). The multi- 515 environmental model predicted extremely high export, but only when [P] was lower than 0.05 μM (Figure 8C, F, I). Second, the effect of tropical [P] levels on $p\text{CO}_{2,\text{atm}}$ was strongly modulated by subtropical [P], reversing from a negative to a positive relationship as subtropical [P] declines (Figure 8I, L). The difference between the nutrient-only model and the multi-environmental model arose because the multi-environmental model 520 incorporated a temperature impact on resource allocation and elemental ratios. Although we were not varying temperature in these experiments, we did represent regional



525

temperatures differences between the different boxes. The result is that a large stoichiometric contrast between the tropical and sub-tropical regions only arose when there was a large difference in nutrient levels between the two regions (Fig. 8L). However, both the nutrient-only model and the multi-environmental model predicted that carbon export and $p\text{CO}_{2,\text{atm}}$ were sensitive to the interaction between regional nutrient availability and $\text{C:P}_{\text{export}}$.



530

Figure 8: Carbon export (Tmol C yr^{-1}) and $p\text{CO}_{2,\text{atm}}$ (ppm) in changing surface phosphate concentrations. Columns correspond to type of stoichiometry; Redfield (Left), nutrient-only (Middle), and multi-environmental model (Right). Rows correspond to either tropical carbon export (A through C), subtropical carbon export (D through F), total carbon export (G through I) or atmospheric $p\text{CO}_2$ (J through L). The grey points represent where $p\text{CO}_{2,\text{atm}}$ was calculated, between spaces are interpolated.



535

3.3 Interactive effect of temperature on stoichiometry, carbon export and atmospheric $p\text{CO}_2$

We next quantified the impact of sea surface T in the tropics and subtropics on $\text{C:P}_{\text{export}}$, carbon export, and $p\text{CO}_{2,\text{atm}}$ (Figure 9A-D). The Redfield model predicts that increases in T lead to a decline in the solubility of CO_2 in seawater and consequently an increase in $p\text{CO}_{2,\text{atm}}$ from 288 to 300 ppm ($\Delta p\text{CO}_{2,\text{atm}} = 12$) (Figure 9A). This feedback was present with the same strength in the nutrient-only model (with no T dependence on C:P), in which $p\text{CO}_{2,\text{atm}}$ ranged from 268 to 280 ppm ($\Delta p\text{CO}_{2,\text{atm}} = 12$) (Figure 9B).

In contrast to the Redfield and nutrient-only models, the temperature-only model predicted a negative linear relationship between $p\text{CO}_{2,\text{atm}}$ and tropical sea surface T and a positive linear relationship between $p\text{CO}_{2,\text{atm}}$ and subtropical sea surface T (Figure 9C). The decline in $p\text{CO}_{2,\text{atm}}$ with tropical sea surface T was driven by an enhancement of export due to increased C:P at higher T 's (Figure 10). At 5°C below modern ocean T , the model predicted C:P in the tropics was 131 and subtropical was 121, resulting in a $p\text{CO}_{2,\text{atm}}$ of 305 ppm. At 5°C above modern ocean T , the model predicted C:P in the tropics is 189 and subtropical was 175, resulting in a $p\text{CO}_{2,\text{atm}}$ of 263 ppm. Tropical T had more impact with $\Delta p\text{CO}_{2,\text{atm}} = 41$ ppm compared to subtropical T 's effect with a $\Delta p\text{CO}_{2,\text{atm}}$ range from 4 to 5 ppm (Figure 10).

Similar to the temperature-only model, the multi-environmental model predicted a negative linear relationship between $p\text{CO}_{2,\text{atm}}$ and tropical sea surface T and a positive linear relationship between $p\text{CO}_{2,\text{atm}}$ and subtropical sea surface T (Figure 9D). The decline in $p\text{CO}_{2,\text{atm}}$ with tropical sea surface T was driven by an enhancement of export due to increased C:P at higher T 's (Figure 10). In the subtropical region, the expected increase in export was mitigated by a decline in solubility. At 5°C below modern ocean T , the trait-based model predicted that C:P in the tropics was 147 and that C:P in the subtropics was 155, resulting in an increase of $p\text{CO}_{2,\text{atm}}$ to 279 ppm (Figure 10). Variation tropical T 's in a 10°C span led to a significant decline in $p\text{CO}_{2,\text{atm}}$, with a $\Delta p\text{CO}_{2,\text{atm}}$ of approximately 46, and tropical C:P ranging from 147 to 210 (Figure 10). Because the subtropical box has a large surface area, the decrease in surface CO_2 solubility at high temperatures is sufficient to overcome the increase in export due to higher C:P leading to a positive relationship between $p\text{CO}_{2,\text{atm}}$ and subtropical temperatures.

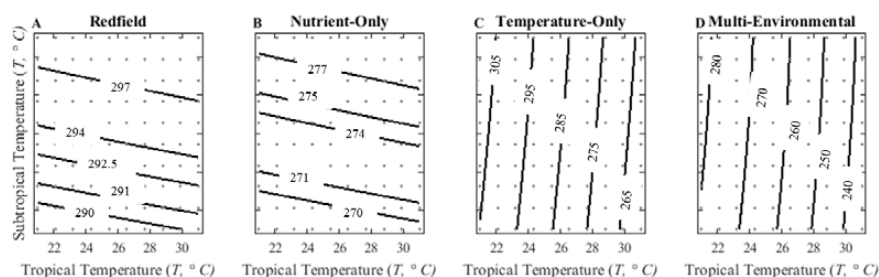


Figure 9: $p\text{CO}_{2,\text{atm}}$ (ppm) as a function of changing surface temperature concentrations. Based on A) Redfield (fixed) stoichiometry model, B) nutrient-only stoichiometry model, C) temperature-only stoichiometry model, and D) multi-environmental stoichiometry model.

570

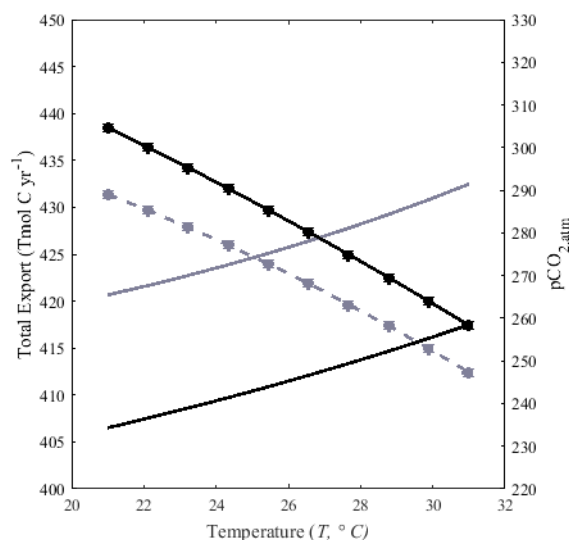


Figure 10: The effect of changing sea surface temperature (°C) on $p\text{CO}_{2,\text{atm}}$ and total carbon export (Tmol C yr^{-1}) in the temperature-only and multi-environmental model. Phosphate concentrations are $0.3 \mu\text{M}$ in the tropical and $0.05 \mu\text{M}$ in the subtropical box. Multi-environmental model total carbon export is the solid gray line, and $p\text{CO}_{2,\text{atm}}$ is the dashed gray line. Temperature-only model total carbon export is the solid black line, and $p\text{CO}_{2,\text{atm}}$ is the dashed black line.

4 Discussion

Here, we found that variable stoichiometry of exported organic material moderates the interaction between low-latitude nutrient fluxes and ocean carbon cycling. A full connecting circulation allows for complete movement of nutrients between ocean regions resulting in strong linkages between nutrient supply ratios and cellular stoichiometric ratios (Deutsch and Weber, 2012). It has been shown that the inclusion of an oceanic circulation connecting high and low-latitude regions results in a feedback effect between high-latitude nutrient export and relative nutrient supply in low-latitudes (Sarmiento et al., 2004; Weber and Deutsch, 2010). Together, the inclusion of lateral transport between ocean regions and of deviations from Redfield stoichiometry within our model led us to predict the existence of strong teleconnections between the iron-limited tropics and the macronutrient limited subtropics. The degree of nutrient drawdown in the tropics had a strongly non-monotonic relationship with $p\text{CO}_{2,\text{atm}}$ because this drawdown influenced both nutrient supply to the subtropics and tropical C:P. The idea of biogeochemical teleconnections has been proposed before, but we found that variations in stoichiometry greatly enhance the importance and strength of such linkages (Sarmiento and Toggweiler, 1984). Thus biome-scale variations in phytoplankton elemental stoichiometry may change the sensitivity of the carbon pump to iron deposition or other phenomena that regulate patterns of nutrient drawdown. We also see that the degree of nutrient drawdown had a strong impact on predicted (and observed) C:P leading to highly non-linear controls on $p\text{CO}_{2,\text{atm}}$ whereby increased export in the tropics counter intuitively leads to increasing $p\text{CO}_{2,\text{atm}}$. This observation suggests that $p\text{CO}_{2,\text{atm}}$ may have a complex link to iron delivery



that is modulated by macro-nutrient availability and phytoplankton resource demand. Thus, large-scale gradients in stoichiometry can alter the regional efficiency of the biological pump: [P] supplied to high C:P regions leads to a larger export of carbon than [P] supplied to low C:P regions, giving an important role to the details of the ocean circulation and other processes that alter nutrient supply and phytoplankton physiological responses in different surface ocean regions. Therefore, biome-scale variations in phytoplankton elemental stoichiometry can lead to a fundamental change in the partitioning of carbon between the atmosphere and the ocean.

Past studies using box models have found $p\text{CO}_{2,\text{atm}}$ to be insensitive to low-latitude nutrients (Follows et al., 2002; Ito and Follows, 2003; Sarmiento and Toggweiler, 1984; Toggweiler, 1999). This phenomena was explored by DeVries and Primeau (2009), who showed that the strength of the thermohaline circulation is the strongest control on $p\text{CO}_{2,\text{atm}}$, and that changes in low-latitude export are relatively unimportant. Unlike our study, such earlier work relied on a uniform Redfield stoichiometry. However, we find that when stoichiometric variation is included, carbon export and $p\text{CO}_{2,\text{atm}}$ become dependent on details of low-latitude processes.

It is important to recognize that a five-box model is an incomplete description of ocean circulation, and is meant only to identify the most important mechanisms, not to make precise quantitative predictions. In order for our model to adequately reflect important features of the carbon and phosphorus nutrient distributions, we had to carefully select the values of the thermohaline and wind-driven upper ocean circulations that lead to reasonable nutrient fluxes and standing stocks. The value of thermocline circulation, T_c , has been calibrated in different box models to range from 12 to 30 Sv (DeVries and Primeau, 2009; Galbraith and Martiny, 2015; Sarmiento and Toggweiler, 1984; Toggweiler, 1999). Representation of the wind driven overturning, T_w , in a simple box model has received less attention. Variations in the thermohaline circulation influence the abundance of nutrients in different boxes. Depending on the strength of this circulation, our model accumulated nutrients in the thermocline box and we tuned this parameter to most accurately mimic nutrient variation across ocean regions. Another caveat relates to our choice of the two-way flux values. Similar to the circulation values, a wide range of two-way flux values have been used in the literature. We therefore performed sensitivity experiments to find the best value for our full model set-up but the qualitative trends observed are insensitive to the choice of such fluxes.

Nutrient availability and temperature have been alternatively proposed as drivers of variation in stoichiometric ratios in the global ocean, and the strong statistical correlation between temperature and nutrients throughout the ocean has prevented identification of the relative importance of each factor. We see that although temperature regulation of $\text{C:P}_{\text{export}}$ can influence $p\text{CO}_{2,\text{atm}}$, this regulation is strongly dependent on the detailed control mechanism and also generally diverge from expectations based on the solubility pump. Our results do not identify whether temperature or nutrient concentrations is the most important driver of phytoplankton C:P, but do suggest that the physiological effect of temperature could be important for ocean carbon cycling. Both the temperature-only and multi-environmental models predict that temperature increases enhance tropical export, causing substantial decreases in $p\text{CO}_{2,\text{atm}}$ with temperature. This relationship is the reverse of that predicted by the nutrient-only and Redfield models, and represents a sizable potential negative feedback on carbon cycling. The multi-



environmental model also predicted that C:P responds in a nonlinear fashion to [P], with significantly increased sensitivity in highly oligotrophic conditions. A deeper understanding of the physiological mechanisms regulating phytoplankton C:P ratios are thus key to understanding the carbon cycle.

Our derivation of the multi-environmental model relies on several important assumptions. The growth rate in the multi-environmental model is determined by a set of environmental conditions and quantified by the specific rate of protein synthesis, carbon fixation and phosphorus uptake. The effect of growth rate on stoichiometry will likely be dependent on whether light, a specific nutrient, or temperature controls growth. The value of specific species of Q_{10} leads to uncertainty in our multi-environmental model because of the range of possible values is highly dependent on the cell or organism being tested. In a study examining Q_{10} of various processes within the cell, it was found that the Q_{10} of photochemical processes ranged from 1.0 to 2.08, and for carboxylase activity of RuBisCO to be 2.66 (Raven and Geider, 1988). In addition to the high uncertainty between Q_{10} values, there is high ambiguity associated with cellular inorganic P stores (e.g., polyphosphates and phospholipids) (Kornberg et al., 1999). P storage, such as polyphosphates, can serve as both energy and nutrient storage that may be regulated by unique environmental factors. Finally, we assume that our choice of the value of Q_{10} for each metabolic process is a potential source of error within our model, because measured values are highly dependent on the cell or organism being tested, and it is difficult to extend these single-organism observations across species. Thus, we recognize multiple caveats within the trait-based model but expect that it improves our ability to link environmental and phytoplankton stoichiometry variation.

5 Conclusions

We find that processes that affect nutrient supply in oligotrophic gyres, such as the strength of the thermohaline circulation, are particularly important in setting $p\text{CO}_{2,\text{atm}}$ but via a complex link with $\text{C:P}_{\text{export}}$. By explicitly modeling the shallow overturning circulation, we showed that increased export in the tropics, which might be influenced by increased atmospheric iron dust deposition, may lead to increases, rather than decreases, in $p\text{CO}_{2,\text{atm}}$. Increased [P] drawdown in the tropics shifts export away from the subtropical gyres, and changes the mean export C:P in the low-latitude ocean. We would expect that nutrient drawdown leads to high export and declines in $p\text{CO}_{2,\text{atm}}$, but instead we find that variation in cellular allocation and adaptation can lead to counterintuitive controls on $p\text{CO}_{2,\text{atm}}$. Additionally, we find that it is even more difficult to separating nutrient supply and temperature controls on marine phytoplankton stoichiometry, carbon export, and $p\text{CO}_{2,\text{atm}}$ and we need better physiological experiments and field data to fully understand the relative impact of the two factors. Nevertheless, it is likely that both play a key role in regulating phytoplankton stoichiometry, $\text{C:P}_{\text{export}}$, and ultimately ocean carbon cycling.

Author Contribution: ARM - creation and analysis of the box model and primary writer of manuscript. GIH - creation and development of the trait-based model, and writing. FWP - assistance on the box model and editing of manuscript of manuscript. SAL - assistance on the trait-based model and editing of manuscript. ACM - assistance on both models and writing of manuscript.



Competing Interests: The authors declare that they have no conflict of interest.

Acknowledgement

695 We thank Alyse Larkin at UCI for many helpful comments. This work was supported by NSF
GRFP to ARM and Biological Oceanography (OCE-1046297 and OCE-1559002) to ACM. GIH
and SAL were supported by NSF Grant OCE-1046001: Dimensions: Biological Controls on
Ocean CNP ratios, NSF Grant GEO-1211972 CNH: Social-Ecological Complexity and
700 Adaptation in Marine Systems, and Simons Foundation Grant 395890 on A New
Framework for Ecological Kinetics in Natural Environments.



Reference

- Van Bogelen, R. A. and Neidhardt, F. C.: Ribosomes as sensors of heat and cold shock in *Escherichia coli*, Proc. Natl. Acad. Sci., 87(15), 5589–5593, doi:10.1073/pnas.87.15.5589, 1990.
- Boyd, P. W. and Trull, T. W.: Understanding the export of biogenic particles in oceanic waters: Is there consensus?, Prog. Oceanogr., 72(4), 276–312, doi:10.1016/j.pocean.2006.10.007, 2007.
- Broecker, W. S.: Ocean chemistry during glacial time, Geochim. Cosmochim. Acta, 47(8), 1539–1540, doi:10.1016/0016-7037(83)90315-0, 1982.
- Broeze, R. J., Solomon, C. J. and Pope, D. H.: Effects of low temperature on in vivo and in vitro protein synthesis in *Escherichia coli* and *Pseudomonas fluorescens*, J. Bacteriol., 134(3), 861–874, 1978.
- Clark, J. R., Daines, S. J., Lenton, T. M., Watson, A. J. and Williams, H. T. P.: Individual-based modelling of adaptation in marine microbial populations using genetically defined physiological parameters, Ecol. Modell., 222(23–24), 3823–3837, doi:10.1016/j.ecolmodel.2011.10.001, 2011.
- Cunningham, B. R. and John, S. G.: The effect of iron limitation on cyanobacteria major nutrient and trace element stoichiometry, Limnol. Oceanogr., doi:10.1002/lno.10484, 2017.
- Daines, S. J., Clark, J. R. and Lenton, T. M.: Multiple environmental controls on phytoplankton growth strategies determine adaptive responses of the N : P ratio., Ecol. Lett., 17, 414–425, doi:10.1111/ele.12239, 2014.
- Deutsch, C. and Weber, T.: Nutrient ratios as a tracer and driver of ocean biogeochemistry, Ann. Rev. Mar. Sci., 4, 113–141, doi:10.1146/annurev-marine-120709-142821, 2012.
- DeVries, T. and Deutsch, C.: Large-scale variations in the stoichiometry of marine organic matter respiration, Nat. Geosci., 7(12), 890–894, doi:10.1038/ngeo2300, 2014.
- DeVries, T. and Primeau, F.: Atmospheric pCO₂ sensitivity to the solubility pump: Role of the low-latitude ocean, Global Biogeochem. Cycles, 23(4), 1–13, doi:10.1029/2009GB003537, 2009.
- Diaz, J. M., Bjorkman, K. M., Haley, S. T., Ingall, E. D., Karl, D. M., Longo, A. F. and Dyhrman, S. T.: Polyphosphate dynamics at Station ALOHA, North Pacific subtropical gyre, Limnol. Oceanogr., 61(1), 227–239, doi:10.1002/lno.10206, 2016.
- Edwards, K., Thomas, M., Klausmeier, C. A. and Litchman, E.: Allometric scaling and taxonomic variation in nutrient utilization traits and maximum growth rate of phytoplankton, Limnol. Oceanogr., 57(2), 554–566, 2012.
- Emerson, S.: Annual net community production and the biological carbon flux in the ocean, Global Biogeochem. Cycles, 28(1), 14–28, doi:10.1002/2013GB004680, 2014.
- Falkowski, P. G. and LaRoche, J.: Acclimation to spectral irradiance in algae, J. Phycol., 27, 8–



- 14, 1991.
- 740 Falkowski, P. G. and Raven, J. a: Aquatic Photosynthesis, Freshw. Biol., 69(10), 375,
doi:10.1016/j.bmcl.2011.05.118, 1997.
- Follows, M. J., Ito, T. and Marotzke, J.: The wind-driven, subtropical gyres and the solubility
pump of CO₂, Global Biogeochem. Cycles, 16(4), 9pp, doi:10.1029/2001GB001786, 2002.
- 745 Galbraith, E. D. and Martiny, A. C.: A simple nutrient-dependence mechanism for predicting
the stoichiometry of marine ecosystems, Proc. Natl. Acad. Sci., 112(27), 201423917,
doi:10.1073/pnas.1423917112, 2015.
- Garcia, H. E., Locarnini, R. A., Boyer, T. P., Antonov, J. I., Baranova, O. K., Zweng, M. M.,
Reagan, J. R. and Johnson, D. R.: World Ocean Atlas 2013: Dissolved Oxygen, Apparent
Oxygen Utilization, and Oxygen Saturation, in NOAA Atlas NESDIS 75., 2014.
- 750 Garcia, N. S., Bonachela, J. A. and Martiny, A. C.: Interactions between growth-dependent
changes in cell size, nutrient supply and cellular elemental stoichiometry of marine
Synechococcus, ISME J, 10(11), 2715–2724 [online] Available from:
<http://dx.doi.org/10.1038/ismej.2016.50>, 2016.
- 755 Geider, R. J., Macintyre, H. L. and Kana, T. M.: A dynamic model of photoadaptation in
phytoplankton, Limnol. Oceanogr., 41(1), 1–15, doi:10.4319/lo.1996.41.1.0001, 1996.
- Goldman, J. C., McCarthy, J. J., Peavy, D. G. and Peavey, D. G.: Growth rate influence on the
chemical composition of phytoplankton in oceanic waters, Nature, 279(5710), 210–215,
1979.
- 760 Henson, S. A., Sanders, R., Madsen, E., Morris, P. J., Le Moigne, F. and Quartly, G. D.: A
reduced estimate of the strength of the ocean's biological carbon pump, Geophys. Res. Lett.,
38(4), 10–14, doi:10.1029/2011GL046735, 2011.
- Ito, T. and Follows, M. J.: Upper ocean control on the solubility pump of CO₂, J. Mar. Res.,
61(4), 465–489, doi:10.1357/002224003322384898, 2003.
- 765 Klausmeier, C. A., Litchman, E., Daufresne, T. and Levin, S. A.: Optimal nitrogen-to-
phosphorus stoichiometry of phytoplankton, Nature, 429(6988), 171–174,
doi:10.1038/nature02454, 2004.
- Kornberg, A., Rao, N. N. and Ault-Riche, D.: Inorganic polyphosphate: A molecule of many
functions, Annu. Rev. Biochem., 68, 89–125, 1999.
- 770 Leonardos, N. and Geider, R. J.: Effects of nitrate: phosphate supply ratio and irradiance on
the C : N : P stoichiometry of *Chaetoceros muelleri*, Eur. J. Phycol., 39(2), 173–180, 2004.
- Leonardos, N. and Geider, R. J.: Elemental and biochemical composition of *Rhinomonas*
reticulata (Cryptophyta) in relation to light and nitrate-to-phosphate supply ratios, J.
Phycol., 41(3), 567–576, 2005.
- 775 Locarnini, R. A., Mishonov, A. V., Antonov, J. I., Boyer, T. P., Garcia, H. E., Baranova, O. K.,
Zweng, M. M., Paver, C. R., Reagan, J. R., Johnson, D. R., Hamilton, M. and Seidov, D.: World



- Ocean Atlas 2013. Vol. 1: Temperature., 2013.
- Martiny, A. C., Vrugt, J. A., Primeau, F. W. and Lomas, M. W.: Regional variation in the particulate organic carbon to nitrogen ratio in the surface ocean, *Global Biogeochem. Cycles*, 27(3), 723–731, doi:10.1002/gbc.20061, 2013a.
- 780 Martiny, A. C., Pham, C. T. A., Primeau, F. W., Vrugt, J. A., Moore, J. K., Levin, S. A. and Lomas, M. W.: Strong latitudinal patterns in the elemental ratios of marine plankton and organic matter, *Nat. Geosci.*, 6(5), 1–5, doi:10.1038/ngeo1757, 2013b.
- Martiny, A. C., Vrugt, J. A. and Lomas, M. W.: Concentrations and ratios of particulate organic carbon, nitrogen, and phosphorus in the global ocean, *Sci. Data*, 1 [online] Available from:
785 <http://dx.doi.org/10.1038/sdata.2014.48>, 2014.
- Mino, T., Van Loosdrecht, M. C. M. and Heijnen, J. J.: Microbiology and biochemistry of the enhanced biological phosphate removal process, *Water Res.*, 32(11), 3193–3207, doi:10.1016/S0043-1354(98)00129-8, 1998.
- Moore, C. M., Mills, M. M., Arrigo, K. R., Berman-Frank, I., Bopp, L., Boyd, P. W., Galbraith, E. D., Geider, R. J., Guieu, C., Jaccard, S. L., Jickells, T. D., La Roche, J., Lenton, T. M., Mahowald, N. M., Maranon, E., Marinov, I., Moore, J. K., Nakatsuka, T., Oschlies, A., Saito, M. A., Thingstad, T. F., Tsuda, A. and Ulloa, O.: Processes and patterns of oceanic nutrient limitation, *Nat. Geosci.*, 6(9), 701–710, doi:10.1038/ngeo1765, 2013.
- 790 Moore, J. K.: Upper ocean ecosystem dynamics and iron cycling in a global three-dimensional model, *Global Biogeochem. Cycles*, 18(4), 1–21, doi:10.1029/2004GB002220, 2004.
- 795 Van Mooy, B. A. S. and Devol, A. K.: Assessing nutrient limitation of *Prochlorococcus* in the North Pacific Subtropical gyre by using an RNA capture method, *Limnol. Oceanogr.*, 53(1), 78–88, 2008.
- 800 Van Mooy, B. A. S., Rocap, G., Fredricks, H. F., Evans, C. T. and Devol, A. H.: Sulfolipids dramatically decrease phosphorus demand by picocyanobacteria in oligotrophic marine environments., *Proc. Natl. Acad. Sci. U. S. A.*, 103, 8607–8612, doi:10.1073/pnas.0600540103, 2006.
- Morel, A. and Bricaud, A.: Theoretical results concerning light absorption in a discrete medium, application to specific absorption of phytoplankton, *Deep. Res.*, 28A, 1375–1393, 1981.
- 805 Mougnot, C., Zimmerman, A. E., Bonachela, J. A., Fredricks, H., Allison, S. D., Van Mooy, B. A. S. and Martiny, A. C.: Resource allocation by the marine cyanobacterium *Synechococcus* WH8102 in response to different nutrient supply ratios, *Limnol. Oceanogr.*, 60(5), 1634–
810 1641, doi:10.1002/lno.10123, 2015.
- Norberg, J., Swaney, D. P., Dushoff, J., Lin, J., Casagrandi, R. and Levin, S. A.: Phenotypic diversity and ecosystem functioning in changing environments: a theoretical framework, *Proc. Natl. Acad. Sci.*, 98(20), 11376–11381, 2001.



- 815 Raven, J. A. and Falkowski, P. G.: Oceanic sinks for atmospheric CO₂, *Plant, Cell & Environ.*, 22(6), 741–755 [online] Available from: <http://dx.doi.org/10.1046/j.1365-3040.1999.00419.x>, 1999.
- Raven, J. A. and Geider, R. J.: Temperature and algal growth, *New Phytol.*, 110(4), 441–461, doi:10.1111/j.1469-8137.1988.tb00282.x, 1988.
- 820 Rhee, G.-Y. and Gotham, I. J.: The effect of environmental factors on phytoplankton growth: Temperature and the interactions of temperature with nutrient limitation, *Limnol. Oceanogr.*, 26(4), 635–648, doi:10.4319/lo.1981.26.4.0635, 1981.
- Rhee, G. Y.: Effects of N-P atomic ratios and nitrate limitation on algal growth, cell composition, and nitrate uptake, *Limnol. Oceanogr.*, 23(1), 10–25, doi:10.4319/lo.1978.23.1.0010, 1978.
- 825 Sarmiento, J. L. and Toggweiler, J. R.: A New Model for the Role of Oceans in Determining the Atmospheric pCO₂, *Nature*, (308), 621–624, 1984.
- Sarmiento, J. L., Gruber, N., Brzezinski, M. a and Dunne, J. P.: High-latitude controls of thermocline nutrients and low latitude biological productivity., *Nature*, 427(6969), 56–60, doi:10.1038/nature10605, 2004.
- 830 Shuter, B.: A model of physiological adaptation in unicellular algae, *J. Theor. Biol.*, 78(4), 519–552, doi:10.1016/0022-5193(79)90189-9, 1979.
- Sigman, D. M. and Boyle, E. A.: Glacial/interglacial variations in atmospheric carbon dioxide, *Nature*, 407(October), 859–869, 2000.
- 835 Sterner, R. W. and Elser, J. J.: *Ecological stoichiometry: the biology of elements from molecules to the biosphere*, Princeton University Press, Princeton, NJ., 2002.
- Talmy, D., Blackford, J., Hardman-Mountford, N. J., Dumbrell, A. J. and Geider, R. J.: An optimality model of photoadaptation in contrasting aquatic light regimes, *Limnol. Oceanogr.*, 58(5), 1802–1818, doi:10.4319/lo.2013.58.5.1802, 2013.
- 840 Talmy, D., Blackford, J., Hardman-Mountford, N. J., Polimene, L., Follows, M. J. and Geider, R. J.: Flexible C : N ratio enhances metabolism of large phytoplankton when resource supply is intermittent, *Biogeosciences*, 11(17), 4881–4895, doi:10.5194/bg-11-4881-2014, 2014.
- Teng, Y.-C., Primeau, F. W., Moore, J. K., Lomas, M. W. and Martiny, A. C.: Global-scale variations of the ratios of carbon to phosphorus in exported marine organic matter, *Nat. Geosci.*, 7(12), 895–898, doi:10.1038/ngeo2303, 2014.
- 845 Thrane, J. E., Hessen, D. O., Andersen, T. and Hillebrand, H.: The impact of irradiance on optimal and cellular nitrogen to phosphorus ratios in phytoplankton, *Ecol. Lett.*, 19(8), 880–888, doi:10.1111/ele.12623, 2016.
- Toggweiler, J. R.: Variation of atmospheric CO₂ by ventilation of the ocean’s deepest water, *Paleo*, 14(5), 571–588, 1999.
- 850 Toseland, A., Daines, S. J., Clark, J. R., Kirkham, A., Strauss, J., Uhlig, C., Lenton, T. M., Valentin,



K., Pearson, G. A., Moulton, V. and Mock, T.: The impact of temperature on marine phytoplankton resource allocation and metabolism, *Nat. Clim. Chang.*, 3(11), 979–984, doi:10.1038/nclimate1989, 2013.

855 Weber, T. S. and Deutsch, C.: Ocean nutrient ratios governed by plankton biogeography., *Nature*, 467(7315), 550–554, doi:10.1038/nature09403, 2010.

Yvon-Durocher, G., Dossena, M., Trimmer, M., Woodward, G. and Allen, A. P.: Temperature and the biogeography of algal stoichiometry, *Glob. Ecol. Biogeogr.*, 24(5), 562–570, doi:10.1111/geb.12280, 2015.